Controller Design Solutions for Long Distance Telesurgical Applications

Tamás Haidegger[1], **Levente Kovács**[1], **Stefan Preitl**[2], **Radu-Emil Precup**[2], **Balázs Benyó**[1] **and Zoltán Benyó**[1]

[1] Laboratory of Biomedical Engineering
Dept. of Control Engineering and Information Technology
Budapest University of Technology and Economics
Magyar tudósok krt. 2., Budapest, 1117, Hungary
{haidegger, lkovacs, bbenyo, benyo}@iit.bme.hu

[2]Dept. of Automation and Applied Informatics
"Politehnica" University of Timisoara
Bd. V. Parvan 2
300223 Timisoara, Romania
{stefan.preitl, radu.precup}@aut.upt.ro

ABSTRACT

Robotic teleoperation has proved to be an effective way to explore remote areas, access dangerous sites, or to provide telepresence. Currently, research projects are pushing the boundaries to develop methods for meaningful health care support through teleoperated robots. Surgical robotics have already shown the feasibility of radical concepts, such as intercontinental surgery, and it is believed that technology will eventually enable to extend its rage to space exploration missions. One of the key problems to tackle is the degrading effect of signal latency on system performance and stability. In this paper, we present a case study investigating solution for handling large delays during real-time teleoperation of a remote surgical robot. Modeling approaches are discussed, and simplified human and machine representations are derived to accommodate long distance telesurgical applications. We have shown that a cascade control structure relying on empirical design can be effectively used in this scenario. A suitable controller was designed based on the extension of Kessler's methods in the inner loop, supported by predictive technique in the outer loop. Several tuning methods resulting in proportional-integral-derivative (PID) controllers in the outer loop are analyzed. This paper suggests the use of PID–fuzzy controllers to improve the control system performance. The proposed cascade loop may be a good solution to support future teleoperational missions.

1 Introduction to medical telerobotics in space

There is an increasing need for teleoperation, as robotic surgery advances on Earth, and communities realize the effectiveness of these systems to extend the reach of modern healthcare to remote areas. The research community has been dealing with space application of telerobotics since the dawn of the field. To cope with the difficulties of endoscopic surgery in weightlessness and the extensive space-system requirements, a three-layered mission architecture was proposed earlier to achieve the highest degree of performance possible by combining robotic and human surgery (Haidegger and Benyo, 2008). Depending on the physical distance between the spacecraft and the ground control center, different telepresence technologies may provide the best performance:

1. Real-time telesurgery: up to 2 s round trip delay; 400,000 km (Earth–Moon distance),

2. Telementoring: up to 50–70 s; 10,000,000 km,

3. Consultancy telemedicine: reaching Mars with 5–44 min latency; 56–399 million km.

The effectiveness of real-time control strategies and communication techniques degrades significantly with the increase of latency. Beyond Earth orbit, radio and microwave frequency signals propagate at almost the speed of light in space, but even in the range of long distance manned space missions, several minutes of latency can be experienced. Special control engineering algorithms have to be applied to extend the feasibility of telesurgery up to a maximum of 2 s of delay. Prior solutions include virtual coupling of the remote environment (Thompson, Ottensmeyer and Sheridan, 1999), predictive displays projecting the intended motion of the tools ahead in time (Rayman, Croome, Galbraith, McClure, Morady, Peterson, Smith, Subotic, Wynsberghe and Primak, 2006). Beyond a few seconds, only semi-real-time mentoring, or off-line consultancy can be given. Our goal was to investigate the possibility of designing a controller that provides a stable and suitable solution for the first zone—near Earth—space telesurgery. We are suggesting also the use of fuzzy logic control as a proportional-integral-derivative (PID)–fuzzy controller to show the importance of artificial intelligence techniques for such applications (Enee and Peroumalnaik, 2008; Joelianto and Ichsan, 2009; Zhao and Hong, 2010).

2 Human Model for Teleoperation Scenarios

2.1 Human operator models

In order to design a suitable control scheme for teleoperation scenarios, it is necessary to derive the applicable model of the human operator (*master*—M) and the robot (*slave*—S). The generally used model of the operator (or pilot) with a first-order neuromuscular lag time model containing simplifications; e.g., neglecting high frequency terms:

$$W_{\mathrm{Op}} = k_{\mathrm{Op}} \frac{(\tau_l s + 1)e^{-s\tau}}{(\tau_i s + 1)(\tau_n s + 1)}, \tag{2.1}$$

where k_{Op} is the operator's static gain, the $e^{-s\tau}$ term reflects the pure time delay caused by the human sensory system limitations, τ_l is the lead time constant (relative rate-to-displacement sensitivity), τ_i is the lag time constant, τ_n the neuromuscular and activation mechanism lag time (McRuer and Jex, 1967).

In many cases, the amplitude ratio data is best approximated with (2.1), called the *crossover model*. The open-loop transfer function with one pole can be derived in the form:

$$W_{\mathrm{Op2}} = k_{\mathrm{Op2}} \frac{\omega_c}{s} e^{-s\tau_d}, \tag{2.2}$$

where k_{Op2} is the static gain, ω_c is the crossover frequency (meaning the limitation of the human operator's reaction based on the information feedback) and τ_d is the delay between the observation and the reaction of the motor system (Rayman, Primak, Patel, Moallem, Morady, Tavakoli, Subotic, Galbraith, van Wynsberghe and Croome, 2005). Rule of thumbs are described in (McRuer, 1995; Hildo, Bijl, 2006) to properly choose ω_c and k_{Op2}.

Assuming zero physiological time delay, (2.2) yields to *Fitts' law* (Fitts, 1992). This is a widely accepted model that describes the time taken to acquire a visual target using some kind of manual input device. In the most generic (Shannon) form, the average time (t) taken to complete the movement is:

$$t = a + b \log_2 \left(1 + \frac{D}{w}\right), \tag{2.3}$$

where a represents the start time, b stands for the inherent speed of the device, D is the distance from the starting point to the center of the target and w is the width of the target measured along the axis of motion (practically, the tolerable error).

3 Robot Model for Teleoperation scenarios

Let us assume that the robot is a series of rigid links with typical mechanical properties, and the servos are driven by the local robot controller according to the control commands from the master side. In telesurgery, it is desirable to minimize the load to the patient's tissue, therefore force control may be used. Commonly, the impedance characteristics of both the master and the slave devices are modeled separately, and the master controllers are very sophisticated and compliant nowadays. A simple dynamic model of the manipulator, incorporating the deviation of the tool from the master controller's position is:

$$\begin{aligned}
\mathbf{f}_{\mathrm{S}} &= k_{\mathrm{S}} \left(\mathbf{x}_{\mathrm{S}}(t) - \mathbf{x}_{\mathrm{M}}\left(t - T_{\mathrm{lat}}\right)\right) \\
&\quad + B_{\mathrm{S}} \left(\dot{\mathbf{x}}_{\mathrm{S}}(t) - \dot{\mathbf{x}}_{\mathrm{M}}\left(t - T_{\mathrm{lat}}\right)\right) + M_{\mathrm{S}}\ddot{\mathbf{x}}_{\mathrm{S}}(t),
\end{aligned} \tag{3.1}$$

where $\mathbf{x}_{\mathrm{S}}$ is the Cartesian position of the slave, $\mathbf{x}_{\mathrm{M}}$ is the Cartesian position of the master, k_{S} is the stiffness of the slave manipulator and T_{lat} is the latency of the communication network (Kawashima, Tadano, Sankaranarayanan and Hannaford, 2008).

Tissue characteristics are considered through Fung's exponential force–stretch ratio curve (Fung, 1990), deriving the relation between Lagrangian stress and stretch ratio:

$$\mathbf{f}_T = p \left(e^{q\,\mathbf{x}_{\mathrm{S}}(t)} - 1\right), \tag{3.2}$$

where p and q are tissue-specific constants, determined to be 0.2 and 400, respectively for in-vivo abdominal tissue (Brouwer, Ustin, Bentley, Sherman, Dhruv and Tendick, 2001). In our target application, strains are low, therefore the tissue behavior can be modeled as linear. $G(s)$ represents the linearized, frequency domain equivalent of (3.2). The slave robot can be modeled together with an observer to determine f_T. Deviation originating from the physical realization of the robot's mechanical structure (imperfections and frictions) have been omitted from the model, resulting the transfer function:

$$W_\mathrm{S} \quad = \quad \frac{(k_\mathrm{S} + B_\mathrm{S}s)\,G(s)}{s\,(M_\mathrm{S}s^2 + B_\mathrm{S}s + k_\mathrm{S} + G(s))}. \tag{3.3}$$

4   Application oriented controller design

4.1   Cascade controller for a telesurgical robot

A realistic teleoperation system suffers from time delays during communications between the master (controller) and slave side (effector system). Unless the process is significantly slower than the latency, the control lag time can cause the deterioration of the control quality and even general instability can occur due to unwanted power generation in the communications. Time-varying delay poses further difficulty to classical PID controllers.

Cascade control can improve control system performance over single-loop control whenever disturbances affect a measurable intermediate/secondary process output that directly modifies the primary process output, or if the gain of the secondary process (including the actuator) is non-linear. Advantages of cascade control have been widely studied and published both for telesurgical and generic space robotic applications (Lantos, 2001; Hirzinger, Heindl and Landzettel, 1989).

4.2   Empirical design approach—Auto-calibration methods

4.2.1   Kessler's methods and their extensions

Based on (2.2), the inner part of the cascade control scheme (robot) can be described in a simple form (Haidegger, Kovács, Preitl, Precup, Kovács, Benyó and Benyó, 2010a). It is well known that empirical methods can provide a solution for automatic calibration, following the mainstream approach of control theory.

As first proposed by Kessler (Kessler, 1958), the class of plants characterized by the transfer function:

$$H_P(s) = \frac{k_P}{s\,(1 + sT_1)\,(1 + sT_\Sigma)}, \tag{4.1}$$

or

$$H_P(s) = \frac{k_P}{s\,(1 + sT_1)\,(1 + sT_2)\,(1 + sT_\Sigma)}, \tag{4.2}$$

can be controlled through empirical methods (Preitl, Precup, Kovacs and Preitl, 2002). In (4.1) and (4.2) T_Σ is a small time constant or aggregated time constant corresponding to the sum of parasitic time constants ($T_\Sigma < T_2 < T_1$). The use of a PI or PID controller having the transfer

function:

$$H_C(s) = \frac{k_c}{s} (1 + sT_{C1}) (1 + sT_{C2}) \qquad (4.3)$$

can ensure acceptable performance (Astrom and Hagglund, 1995). T_Σ can also include the time constants used to approximate the time delay. In (4.2), the process pole ($p_1 = -1/T_1$) may be compensated by the controller zero ($z_1 = -1/T_{C2}$) in order to obtain the desired open-loop $H_0(s)$ transfer function in the form:

$$H_0(s) = H_C(s)H_P(s) = \frac{k_0 (1 + sT_{C1})}{s^2 (1 + sT_\Sigma)}, \qquad (4.4)$$

with $k_0 = k_c k_P$.

Extensions of the Kessler methods were proposed in the literature (Preitl and Precup, 1999; Vrancic, Strmcnik and Juricich, 2001), and the *Extended Symmetrical Optimum method* (ESO) was derived (Preitl and Precup, 1999), where:

$$k_c = \frac{1}{k_P \beta^{\frac{3}{2}} T_\Sigma^2}, \ T_{C1} = \beta T_\Sigma \ \text{and} \ T_{C2} = T_1. \qquad (4.5)$$

Tuning parameters are directly correlated to the desired control system performance indices. The value of β is typically chosen to be in the $[4 \ldots 20)$ interval (Preitl and Precup, 2003). It is possible to optimize β for maximum Phase Margin (PM) for any given k_P constant. Depending on β, the closed loop systems poles (p_1, p_2, p_3) can be (Preitl and Precup, 2000):

- $p_{1,2}$ are complex conjugated, if $\beta < 9$,

- $p_{1,2,3}$ are real and equal, if $\beta = 9$,

- all poles are real and distinct for $\beta > 9$, but the system remains oscillatory.

The open loop transfer function can be given as:

$$H_0(s) = \frac{1 + \beta T_\Sigma s}{\beta^{\frac{3}{2}} T_\Sigma^2 s^2 (1 + T_\Sigma s)}. \qquad (4.6)$$

5 Controller Design Solutions for Long Distance Telesurgery

Considering the discussed challenges, we were focusing on classical control options to provide a simple, universal and scalable solution (Haidegger, Kovács, Preitl, Precup, Kovács, Benyó and Benyó, 2010b). In the case of a cascade structure, the data of the inner loop gives feedback to the outer loop, but no a priori knowledge about the inner loop's dynamics is required to design the outer controller. On the other hand, it is possible to explicitly consider the remote dynamics in the outer controller in order to predict the inner behavior (Arcara and Melchiorri, 2002). This can be based on the well-known *Smith predictor* scheme, or similar predictors (Lantos, 2001; Alvarez-Aguirre, 2010).

Fig.1 shows the schematic block diagram of the controller structure. It is important to identify the right model of each component and to define the required parametric filtering enabling the smooth handling of the whole cascade structure.
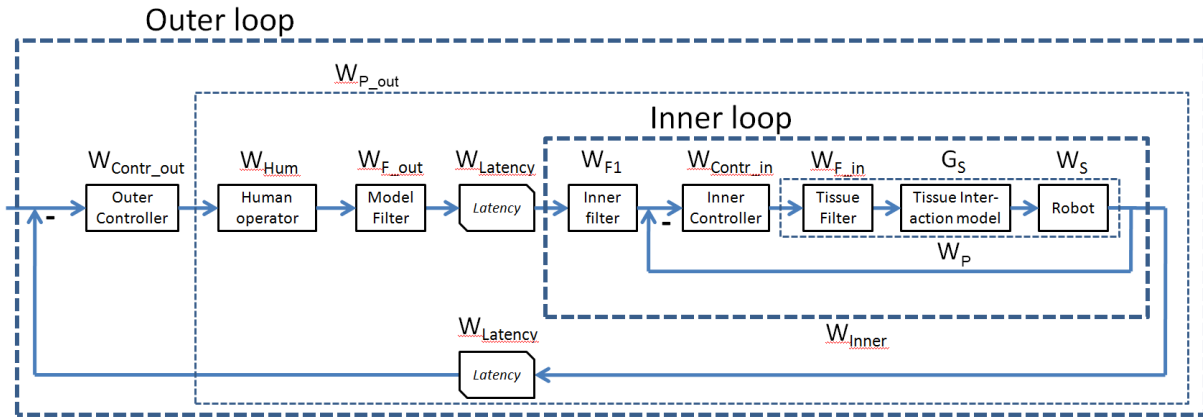
Figure 1: The concept of applying cascade control to deal with extreme latencies in telesurgery.

A predictor in the outer loop helps to deal with the computation of the delayed information from the inner part, whereas a classical PID controller is implemented at the inner part. This is a crucial and effective observation, as in case of teleoperating a robot in a spacecraft, significant delays appear in the control loop. The use of empirical design methods is justified with the need for simple and quick algorithms in cases when model predictive control may be cumbersome to apply. In fact, a human physician controls the robot, and it is extremely difficult to develop plausible model for their behavior from the control point of view. Our goal was to give a scalable solution for the first phase of advanced telesurgical support (Haidegger and Benyó, 2007) based on classical control theory. We focused on Kessler's Extended Symmetrical Optimum method and developed its first embedded application in the broader domain of robotics.

5.1   Realization of control methods

The above presented telesurgery support method has been tested in simulations to show its effectiveness. The models for teleoperation have been defined and implemented under MATLAB R2009b and Simulink 7.1 environment.

Master–slave robots are typically used in a discrete position-controlled mode, therefore the use of step function for excitation during evaluation is suitable to analyze the performance of different controllers. While robot parameters are given in SI units below, the step function's amplitude/time diagrams scale down proportionally, as a robot would not move faster than 100 mm/s, while in the low level control, it must be regulated with 1–10 kHz control cycle. During the evaluation, a critical factor was to ensure that the PM is between 45–60°, where the system is inherently stable, and we also set requirements for reasonable performance in terms of overshoot (σ), the absolute maximum of the signal and settling time (τ_t), the time by the signal reaches the $\pm 2\%$ proximity of its final value.

5.2 Slave side—inner loop

The slave robot can be modeled in accordance with (3.3):

$$W_S = \frac{(k_S + B_S s) G(s)}{s (M_S s^2 + B_S s + k_S + G(s))}. \tag{5.1}$$

The tissue model in s domain (assuming constant contact force) is:

$$G(s) = p \left(e^{qK} - 1\right) = \frac{k_t}{s}. \tag{5.2}$$

However, when $K = x_S(t)_{\text{const}}$, substituting $G(s)$ into (5.1), the plant's transfer function becomes:

$$W_P = \frac{k_t B_S s + k_t k_S}{s (M_S s^2 + B_S s + (k_S + k_t))} \tag{5.3}$$

Assuming a reasonably small slave robot that might be suitable for long duration space missions based on (Kawashima et al., 2008): M_S = 0.1 kg, B_S = 20 Ns/m, k_S = 400 and x_S = 0.001 m. Tissue interaction parameters were chosen similarly: p = 0.2 and q = 400.

First, let us employ an input filter on the plant:

$$W_{\text{F\_in}} = \frac{1}{\frac{B_S}{k_S s + 1}}, \tag{5.4}$$

leading to a filtered plant in the form of (4.1), with:

$$k_P = \frac{k_S k_t}{k_S + k_t} = 0.0938, \tag{5.5}$$

$$T_1 = \frac{2(k_S + k_t)}{B_S - \sqrt{B_S^2 - 4M_S(k_S + k_t)}} = 0.0444s \text{ and} \tag{5.6}$$

$$T_\Sigma = \frac{2(k_S + k_t)}{B_S + \sqrt{B_S^2 - 4M_S(k_S + k_t)}} = 0.0056s. \tag{5.7}$$

Good control system performance indices (*overshoot, settling time, control error*) can be obtained with a PID controller applied to the inner control loop having the transfer function:

$$W_{\text{Contr\_in}} = \frac{k_{\text{Contr\_in}}}{s}(1 + sT_{\text{C1}})(1 + sT_{\text{C2}}). \tag{5.8}$$

The following tuning equations—specific to ESO method—lead to the tuning parameters of the PID controller in the inner loop:

$$k_{\text{Contr\_in}} = \frac{1}{\beta^2 \sqrt{\beta} k_P T_\Sigma^2}, \ T_{\text{C1}} = T_1, \ T_{\text{C2}} = \beta T_\Sigma, \tag{5.9}$$

where $\beta = \beta_{\text{Inner}}$ is the tuning parameter of the inner control loop. The designer can set the value of this parameter to ensure an acceptable compromise in the control system performance indices.

The open-loop and closed loop transfer functions (W_0 and W_C, respectively) derive to be:

$$\begin{aligned} W_0 &= W_{\text{PF}} W_{\text{Contr\_in}} \text{ and} \\ W_C &= \frac{W_0}{1 + W_0} = \frac{1 + \beta T_\Sigma s}{(1 + \sqrt{\beta} T_\Sigma s)\left[1 + (\beta - \sqrt{\beta})T_\Sigma s + \beta T_\Sigma^2 s^2\right]}. \end{aligned} \tag{5.10}$$
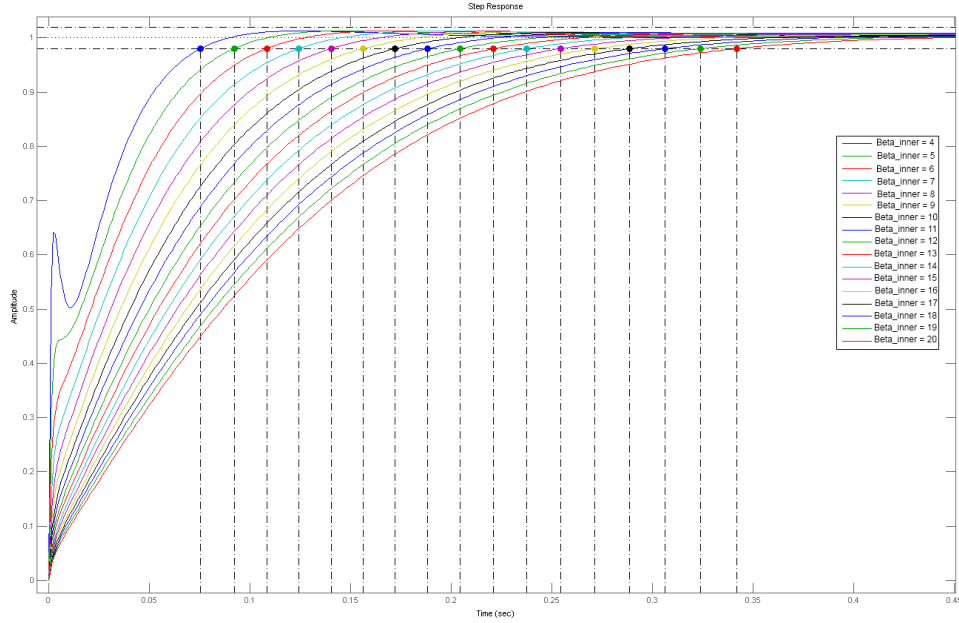
Figure 2: Step response of the filtered, closed loop W_{Inner} system.

For $\beta = [4, 9]$, W_0 contains a complex conjugated pole pair, with slightly decreasing absolute values. Therefore it is advisable to apply filtering in accordance with (Preitl and Precup, 1999). Filtering for $p_{1,2}^*$ means to compensate for the complex conjugated poles in the $\beta = [4, 9]$ domain.

$$W_{\text{F1}} = \frac{1 + \left(\beta - \beta^{\frac{1}{2}}\right) T_\Sigma s + \beta T_\Sigma^2 s^2}{(1 + \beta T_\Sigma s)(1 + \lambda T_\Sigma s)}, \quad \text{where } \lambda = \beta - \beta^{\frac{1}{2}} - 1. \tag{5.11}$$

Then the W_{F1} filter is applied, and the closed loop transfer function of the inner control loop (W_{Inner}) becomes:

$$W_{\text{Inner}} = W_{\text{F1}} W_C = \frac{1}{(1 + T_{\text{P1}}s)(1 + \lambda T_{\text{P2}}s)}, \tag{5.12}$$

where $T_{\text{P1}} = \sqrt{\beta} T_\Sigma$ and $T_{\text{P2}} = T_\Sigma$.

Based on the data presented in Table 1, β_{Inner} must be over 5 to ensure $45°$ PM, resulting in inherent stability of the system. Overshoot is 0% in every case due to the fact that we employed a (5.11) type filter (Fig.2). Based on the experiments, it is advantageous to choose $\beta_{\text{Inner}} = 6$ for further design calculations, ensuring the best performance. This allows for 12 Hz control cycle (comparable to the performance of current optical tracking systems). The inner loop PID controller's parameters for $\beta_{\text{Inner}} = [4 \dots 16]$ are:

- $k_{\text{Contr\_in}} = 4002.6 \dots 5003.3$,

- $T_{\text{C1}} = 0.0444$ (for every β_{Inner}),

- $T_{\text{C2}} = 0.0225 \dots 0.0902$.

Table 1: Controller performance parameters for the inner loop with different β_{Inner} settings

β	Phase Margin	Overshoot	Settling time
4	36.9°	0%	0.052 s
5	41.8°	0%	0.066 s
6	**45.6°**	**0%**	**0.082 s**
7	48.6°	0%	0.099 s
8	51.1°	0%	0.117 s
9	53.1°	0%	0.135 s
10	54.9°	0%	0.154 s
11	56.4°	0%	0.173 s
12	57.8°	0%	0.192 s
13	59°	0%	0.212 s
14	60.1°	0%	0.231 s
15	61°	0%	0.251 s
16	61.9°	0%	0.271 s

5.3 Master side—outer loop

The human operator's model (W_{Hum}) in accordance with the crossover model (2.2) can be modelled using *Padé approximation* (Lantos, 2001):

$$W_{\text{Hum}} = k_{p\_\text{Hum}} \frac{\omega_{c\_\text{Hum}}}{s} e^{-sT_{\text{Hum}}} \approx W_{\text{Hum\_Padé}} = k_{p\_\text{Hum}} \frac{\omega_{c\_\text{Hum}}}{s} \frac{2 - sT_{\text{Hum}}}{2 + sT_{\text{Hum}}}, \tag{5.13}$$

where T_{Hum} represents the human operator's physiological latency. Typically, T_{Hum} = 0.1 s and $k_{p\_\text{Hum}}\omega_{c\_\text{Hum}}$ = 1.

Filtering in the outer loop can be used to speed up the system. We compensate for the denominator of the inner closed loop transfer function in (5.12). The transfer function of the outer loop filter is:

$$W_{\text{F\_out}} = \frac{1 + sT_{\text{Comp}}}{1 + sT_F}, \tag{5.14}$$

where T_F is a filter time constant. T_{Comp} is set to compensate for the largest time constant in (5.12):

$$T_{\text{Comp}} = \max\left(T_{P1}, T_{P2}\right), \text{ therefore} \tag{5.15}$$

$$T_{\text{Comp}} = \max\left(\sqrt{\beta}T_\Sigma, \lambda T_\Sigma\right) = \begin{cases} \sqrt{\beta}T_\Sigma & \text{if} \quad 1 < \beta \le 3 + 2\sqrt{2} \\ \lambda T_\Sigma = (\beta - \sqrt{\beta} - 1)T_\Sigma & \text{if} \quad \beta > 3 + 2\sqrt{2} \end{cases}$$

In addition, T_F is a small filter time constant fulfilling the condition:

$$0 < T_F \ll \min\left(\sqrt{\beta}T_\Sigma, \lambda T_\Sigma\right) = T_{P3}. \tag{5.16}$$

The transfer function of the outer loop process is derived using notation T_m for time delay: $T_m = T_d + T_{\text{Hum}}$, where T_d is the round-trip latency.

$$
\begin{aligned}
W_{\text{P\_out}} &= W_{\text{Hum}} W_{\text{F\_out}} W_{\text{Latency}} W_{\text{Inner}} W_{\text{Latency}} = \frac{k_{\text{P\_out}}}{s(1+sT_F)(1+sT_{\text{P3}})} e^{-sT_m}, \\
k_{\text{P\_out}} &= k_{\text{P\_Hum}} \omega_{\text{c\_Hum}}, \\
T_m &= T_{\text{Hum}} = 2T_d.
\end{aligned}
\tag{5.17}
$$

This transfer function can be used in the design and tuning of the outer loop controller with transfer function $W_{\text{Contr\_out}}$. The open-loop and closed loop transfer functions, W_{0_out} and $W_{\text{C\_out}}$ are:

$$
\begin{aligned}
W_{0\_\text{out}} &= W_{\text{Contr\_out}} W_{\text{P\_out}} \text{ and} \\
W_{\text{C\_out}} &= \frac{W_{0\_\text{out}}}{1 + W_{0\_\text{out}}}.
\end{aligned}
\tag{5.18}
$$

Using (5.16), a simplified version of the transfer function in (5.17) can be derived:

$$
W_{\text{P\_out}} \approx \frac{k_{\text{P\_out}}}{s(1 + T_{\text{P\_out}})} e^{-sT_m}, \quad \text{where } T_{\text{P\_out}} = T_F + T_{P2}.
\tag{5.19}
$$

Using Padé approximation, the transfer function of the outer loop process is approximated as:

$$
\begin{aligned}
W_{\text{P\_out}} \approx W_{\text{P\_out\_Padé}} &= W_{\text{Hum\_Padé}} W_{\text{F\_out}} W_{\text{Padé}} W_{\text{Inner}} W_{\text{Padé}} = \\
&= \frac{k_{\text{P\_out}}(1 - sT_{\text{Hum}}/2)(1 - sT_d/2)^2}{s(1 + sT_F)(1 + sT_{\text{P3}})(1 + sT_{\text{Hum}}/2)(1 + sT_d/2)^2}.
\end{aligned}
\tag{5.20}
$$

5.4 Classical solutions to handle time delay in telesurgery

Next, we discuss plausible options to deal with the outer controller design. Different approaches have been considered, simulated and evaluated to determine their usability in the given cascade structure for teleoperation.

5.4.1 Case 0: Empirical approach through extended Ziegler–Nichols method

A classical controller tuning method was described by *Ziegler and Nichols* (Z–N) (Ziegler and Nichols, 1942). In the case of the above described cascade system, a PID controller for the outer loop—consisting of the entire slave side and the human operator—can be designed applying Z–N. It needs a practical extension to handle a generic system ($W_{\text{P\_out}}$) having the transfer function (5.19). A PID controller in the form of:

$$
W_{\text{Contr\_out}} = \frac{k_{\text{Contr\_out}}}{s}(1 + sT_{\text{C1\_out}})(1 + sT_{\text{C2\_out}})
\tag{5.21}
$$

can be designed using the following parameters:

$$
\begin{aligned}
k_{\text{Contr\_out}} * k_{\text{P\_out}} * \rho &\leq 1.2, \\
\rho &= \frac{T_m}{T_{\text{P\_out}}}, \\
T_{\text{C1\_out}} &= 2T_m \text{ and} \\
T_{\text{C2\_out}} &= T_m.
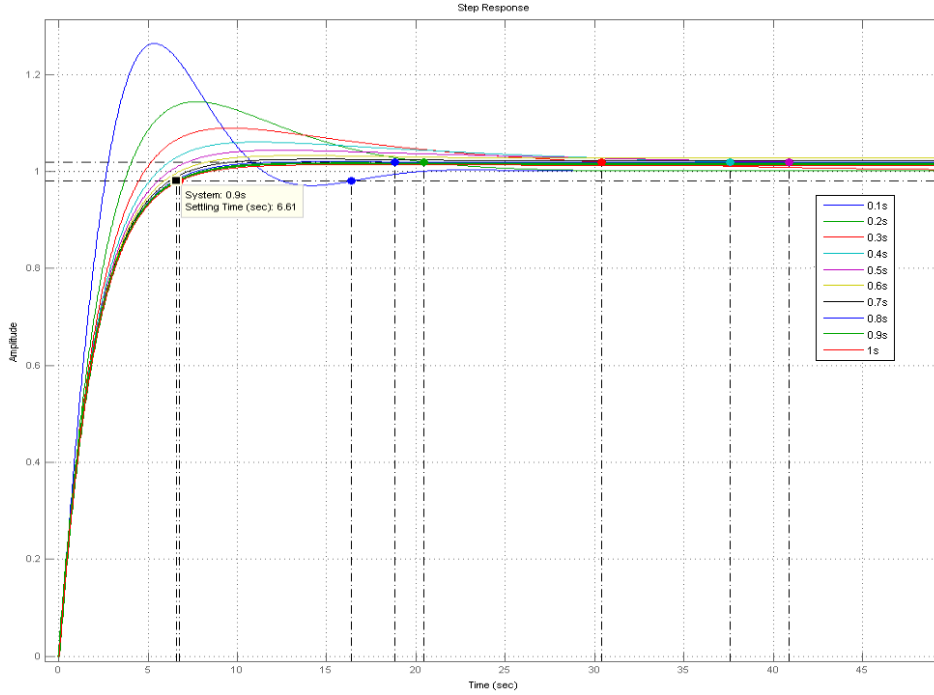\end{aligned}
\tag{5.22}
$$

Figure 3: Step response of the closed loop system with different latencies $0.1 \dots 1$ s. Experiments showed that the Ziegler–Nichols method results in very slow systems.

For the surgical teleoperation system $T_m = T_d + T_{\text{Hum}}$. The extension means we handle the model of the human operator with the given parameters as a latency within the system. Then, the Z–N method can be applied to (5.17).

Performing simulations for the system, the Z–N method offers stable controllers for different possible β_{Inner} parameters of the inner loop, but with very low PM, therefore large oscillations. The method creates very slow systems for even moderate latencies (< 1 s), as shown in Fig. 3, therefore it can be stated that the Z–N method fails to provide a universal solution to the control problem of delayed teleoperation.

The outer loop PID controller's parameters for $T_d = [0.2 \dots 2]$ s are:

- $k_{\text{Contr\_out}} = 0.113 \dots 0.016$,

- $T_{\text{C1\_out}} = 0.6 \dots 4.2$,

- $T_{\text{C2\_out}} = 0.3 \dots 2.1$.

5.4.2 Case 1: Straight application of Kessler's method

Originally, the transfer function of a plant applicable to Kessler's method does not include latency, as shown in (4.1), (4.2). Delays in the system must be approximated and handled in an aggregated manner, as derived in (5.20). The plan is therefore:

$$W_{\text{P\_out}} = \frac{k_{\text{P\_out}}}{s(1 + T_{\text{P\_out}})} e^{-sT_m}, \text{ where } T_{\text{P\_out}} = T_F + T_{P2}, \tag{5.23}$$

Table 2: Maximum latency manageable with different β_{Inner} design parameter settings in the inner loop's controller.

β_{Inner}	4	**5**	**6**	7	8	9	10	11	12	13	14	15	16
$T_{d_{\max}}[s]$	0.016	**0.028**	**0.022**	0.016	0.011	0.005	0	0	0	0	0	0	0

and the PID controller is defined in the form:

$$W_{\text{Contr\_out}} = \frac{k_{\text{Contr\_out}}}{s}(1 + sT_{\text{C1\_out}})(1 + sT_{\text{C2\_out}}), \tag{5.24}$$

and applying the tuning parameters of the PID controller similarly to the inner loop in (5.9):

$$k_{\text{Contr\_out}} = \frac{1}{\beta^2\sqrt{\beta}k_{\text{P\_out}}T_\Sigma^2}, \ T_{\text{C1\_out}} = T_1, \ T_{\text{C2\_out}} = \beta T_\Sigma, \tag{5.25}$$

where $\beta = \beta_{\text{Outer}}$ is the tuning parameter of the outer control loop.

Without distorting the effectiveness of Kessler's method, we can employ Padé approximation for latencies not effecting the largest time constant of the original plant:

$$T_{\text{Pl}} \geq \overbrace{(T_d + T_{\text{P2}})}^{T_\Sigma}, \tag{5.26}$$

where T_{Pl} is the largest time constant of the process, T_d is the time delay and T_{P2} being the aggregation of the smaller time constants. Then we can apply the method analogous to (5.20), using a PID controller having the transfer function:

$$W_{\text{Contr\_out}} = \frac{k_{\text{Contr\_out}}}{s}(1 + sT_{\text{C1\_out}})(1 + sT_{\text{C2\_out}}). \tag{5.27}$$

Depending on the β_{Inner} scaling factor applied in the inner loop, the time constants of the outer loop will vary, therefore different amount of latency can be handled this way. We could show based on Table 2 that to achieve maximum latency handling $\beta_{\text{Inner}} = 5$ provides the highest value, while respecting (5.26). However, as presented in Table 1, stability of the inner loop is only guaranteed with higher β_{Inner}, therefore $\beta_{\text{Inner}} = 6$ is the optimal choice.

With this assumption, latency in the system can be handled. Let us consider the previously discussed robotic teleoperational setup, where the time constants of the outer loop transfer function denominator are $T_{\text{Outer}} = [0.05, 0.0138, 0.0144]$ s, therefore let us build an approximated transfer function with time constants:

$$T_{\text{Pl}} = 0.05 \text{ and}$$
$$T_\Sigma = \overbrace{(0.0138 + 0.0144)}^{0.0282}. \tag{5.28}$$

In terms of (5.26), a maximum of 0.0218 s latency can be tolerated by this design mode. Applying $T_d = 0.0218$ to the simulations, the resulting stable controller's performance is shown in Fig.4. The controller's parameters for $\beta_{\text{Outer}} = [4 \dots 16]$ are:
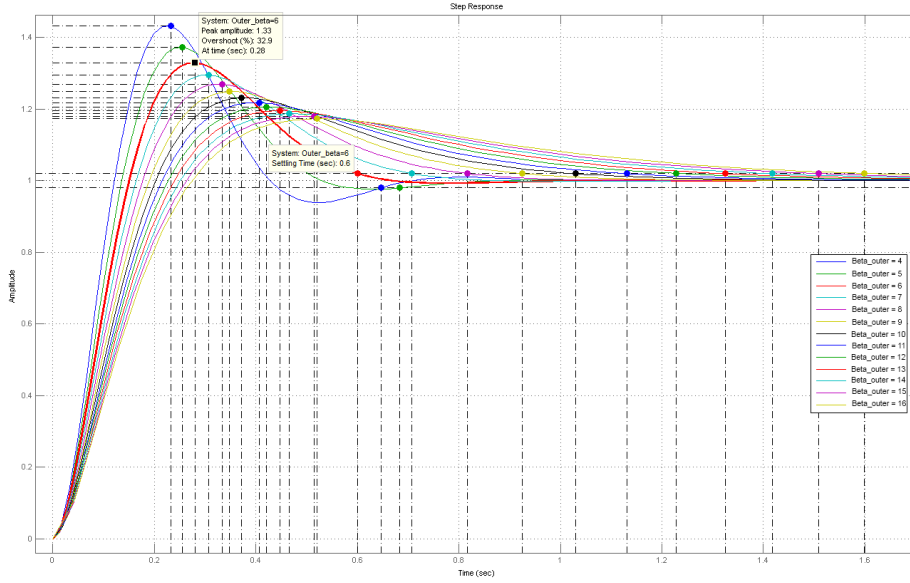
- $k_{\text{Contr\_out}} = 81.862 \dots 10.233$,

Figure 4: Step response of the whole closed loop system with different β_{Outer} settings (classical ESO) and a maximum of 0.0218 s communication lag time. Kessler's classical method was employed for controller design.

- $T_{\text{C1\_out}} = 0.05$,

- $T_{\text{C2\_out}} = 0.156 \ldots 0.625$.

This results in a slow controller (with $\tau_{\min} = 0.6$ s settling time) with significant ($\sigma = 33\%$) overshoot. Clearly, this method has a major limitation towards latency handling, and further design consideration are to be made to enable the tolerance of higher latencies, as discussed below.

5.4.3 Case 2: Stretching Kessler's robustness

It is possible to overcome the limitation of the above mentioned setup by violating condition (5.26). While the extended Kessler method (Preitl and Precup, 1999) only guarantees over-shoot and settling parameters if the largest time constraint is compensated, the robustness of the design method can be exploited. For the plant defined in (5.19):

$$W_{\text{P\_out}} = \frac{k_{\text{P\_out}}}{s(1 + T_{\text{P\_out}})} e^{-sT_m}, \text{ where } T_{\text{P\_out}} = T_F + T_{P2}, \tag{5.29}$$

with the PID controller:

$$W_{\text{Contr\_out}} = \frac{k_{\text{Contr\_out}}}{s}(1 + sT_{\text{C1\_out}})(1 + sT_{\text{C2\_out}}), \tag{5.30}$$

and applying the tuning parameters of the PID controller similarly to the inner loop in (5.9):

$$k_{\text{Contr\_out}} = \frac{1}{\beta^2\sqrt{\beta}k_{\text{P\_out}}T_\Sigma^2}, \ T_{\text{C1\_out}} = T_1, \ T_{\text{C2\_out}} = \beta T_\Sigma, \tag{5.31}$$

this will return the same results as the previous (classical) method for $T_d \leq 0.0218$, but will also give stable solutions for larger latencies. Using the same PID structure (5.21), the controller's parameters for $\beta_{\text{Outer}} = 6$ and $T_d = [0.2 \ldots 2]$ s are:

- $k_{\text{Contr\_out}} = 11.133 \ldots 0.2439$,

- $T_{\text{C1\_out}} = 0.05$,

- $T_{\text{C2\_out}} = 0.469 \ldots 3.169$.

Fig.5(a,b) show the results for T_d = 0.1, the step response and Bode plot for $\beta_{\text{Outer}} = [4, 16]$ values. β_{Inner} was set to the optimal value, 6. The best results were acquired at β_{Outer} = 6, where σ = 33% and τ = 1.28 s. The PM is increasing along with β_{Outer}, as the system is getting slower and slower due to the nature of combined time constant approximation. With increasing time delay, only the settling time grows (Fig.5c). For the desired maximum design constraint of 1 s latency (with β_{Outer} = 6), this method gives σ = 33% and τ = 8.11 s, which is unacceptable for teleoperational application.

It is also possible to test the robustness of Kessler's method through not incorporating the latency in T_σ. In this case, applying the previous β settings, the controller designed will be unstable. However, the extreme choice of the parameters ($\beta_{\text{Inner}} = \beta_{\text{Outer}}$ = 16) leads to a stable controller for up to 0.5 s through slowing down the system, as shown in Fig.6. In fact, latency over 0.2 s results in an under-damped system.

This analysis leads to the conclusion that better method is required to reach the 2 s round-trip latency range with a safe and effective controller design.

5.4.4   Case 3: Kessler's method with Smith predictor

Smith predictor is a model based prediction method which handles the time delay outside of the control loop and allows a feedback design based on a delay-free system (Lantos, 2001). For a generic system having the transfer function:

$$W_{\text{P}} = W_{\text{P}} e^{-sT_d}, \tag{5.32}$$

where T_d is the latency and the $W_{\text{P}}(s)$ plant transfer function is assumed to be open-loop stable, the closed loop transfer function derives to be:

$$W_C = \frac{W_{\text{C}} W_{\text{P}}}{1 + W_{\text{C}} \tilde{W}_{\text{P}} + W_{\text{C}}(W_{\text{P}} e^{-sT_d} - \tilde{W}_{\text{P}} e^{-s\tilde{T}_d})} e^{-sT_d}, \tag{5.33}$$

where $\tilde{W}_{\text{P}}$ is the model of the plant and $\tilde{T}_d$ is the approximation of the time delay. When these models match perfectly, the closed loop transfer function becomes:

$$W_C = \frac{W_{\text{C}} W_{\text{P}}}{1 + W_{\text{C}} W_{\text{P}}} e^{-sT_d}. \tag{5.34}$$

Applying this to $W_{\text{P\_out}}$ defined in (5.17):

$$W_{\text{C\_out}} = \frac{W_{\text{Contr\_out}} W_{\text{P\_out}}}{1 + W_{\text{Contr\_out}} W_{\text{P\_out}}} e^{-sT_d}. \tag{5.35}$$
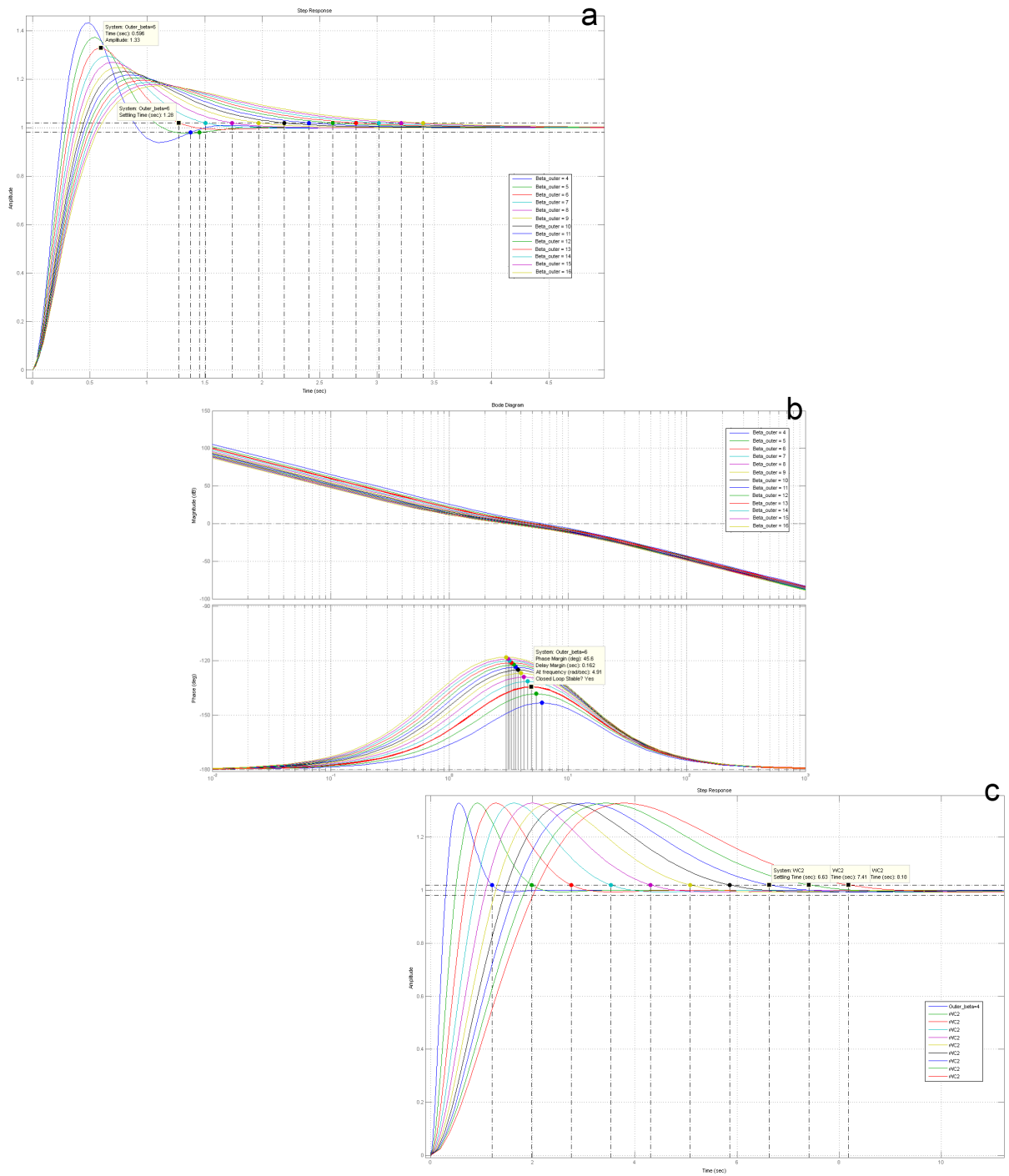
Figure 5: a) Step response of the whole closed loop system with different β_{Outer} settings employing the stretched version of Kessler's method. T_d was 0.1 s. b) Bode plot of the system with the same settings. c) Step response of the system with $\beta_{\text{Inner}} = \beta_{\text{Outer}} = 6$ and T_d = 0.1–1 s.
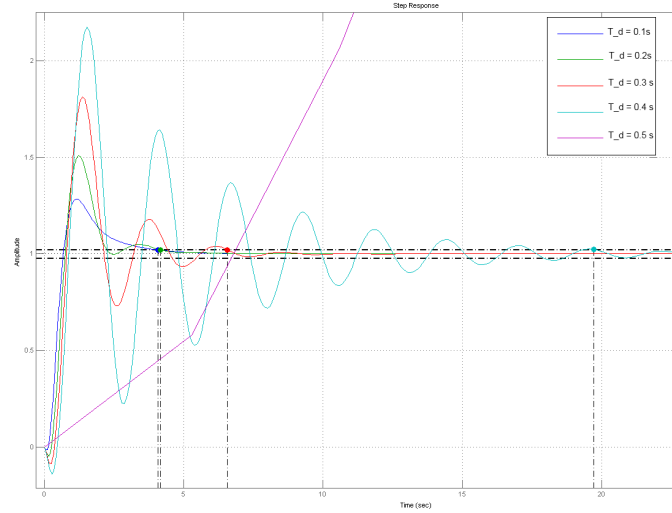
Figure 6: The robustness of Kessler's method proven through its ability to compensate for latencies up to 0.5 s, originally not incorporated in the system model.

Similar conditions have been simulated than before, and in the case of $T_d = 0.1$ s, the deriving system performs better than in the previous cases. Table 3 summarizes the numeric results for $\beta_{\text{Inner}} = 6$, employing 5th order Padé approximation for the latency. The plan is:

$$W_{\text{P\_out}} = \frac{k_{\text{P\_out}}}{s(1 + T_{\text{P\_out}})} e^{-sT_m}, \text{ where } T_{\text{P\_out}} = T_F + T_{P2}, \tag{5.36}$$

and the PID controller is:

$$W_{\text{Contr\_out}} = \frac{k_{\text{Contr\_out}}}{s}(1 + sT_{\text{C1\_out}})(1 + sT_{\text{C2\_out}}), \tag{5.37}$$

with tuning equations of the PID controller, just as like before:

$$k_{\text{Contr\_out}} = \frac{1}{\beta^2\sqrt{\beta}k_{\text{P\_out}}T_\Sigma^2}, \ T_{\text{C1\_out}} = T_1, \ T_{\text{C2\_out}} = \beta T_\Sigma, \tag{5.38}$$

It can be seen that $\beta_{\text{Outer}} = 9$ gives the best results along the pre-defined criteria.

With this controller structure, it is finally possible to properly address the issues with large latencies (e.g., $T_d = 2$ s, as targeted before). To ensure the smooth hold phase of the system, higher order ($>$5[th]) Padé approximation was used. This also increased the overshoot, therefore a rational compromise was chosen. From the application point of view, the amplitude of the oscillation (A_{max}) during the hold phase can be critical, thus it is a limiting factor regarding the choice of order and the overshoot. It has been determined to only allow a maximum of 10% overshoot during the hold phase, therefore bigger ($>$15th) order Padé approximation should be used based on Table 4.

Previous considerations for β are valid here as well, therefore $\beta_{\text{Inner}} = 6$ provides a rational compromise between rise-time and overshoot. With 15th order Padé approximation the effect of the $\beta_{\text{Outer}} = [4, 16]$ parameter on the system is shown in Fig. 7, using the same PID controller structure (5.21). The smoothing effect of higher β in return of slowing down the system is displayed numerically in Table 5. The optimal parametrization of the control structure for extreme

Table 3: Controller performance parameters for Case 3 with different β_{Outer} settings

β_{Outer}	Phase Margin	Overshoot	Settling time
4	41°	43%	0.57 s
5	41.5°	37%	0.54 s
6	42.3°	33%	0.47 s
7	43.3°	30%	0.61 s
8	44.3°	27%	0.69 s
9	**45.3°**	**25%**	**0.77 s**
10	46.2°	23%	0.84 s
11	47.1°	22%	0.92 s
12	47.9°	21%	0.99 s
13	48.7°	20%	1.06 s
14	49.4°	19%	1.12 s
15	50.1°	18%	1.19 s
16	50.8°	17%	1.26 s

Table 4: Effect of order of Padé approximation on control parameters.

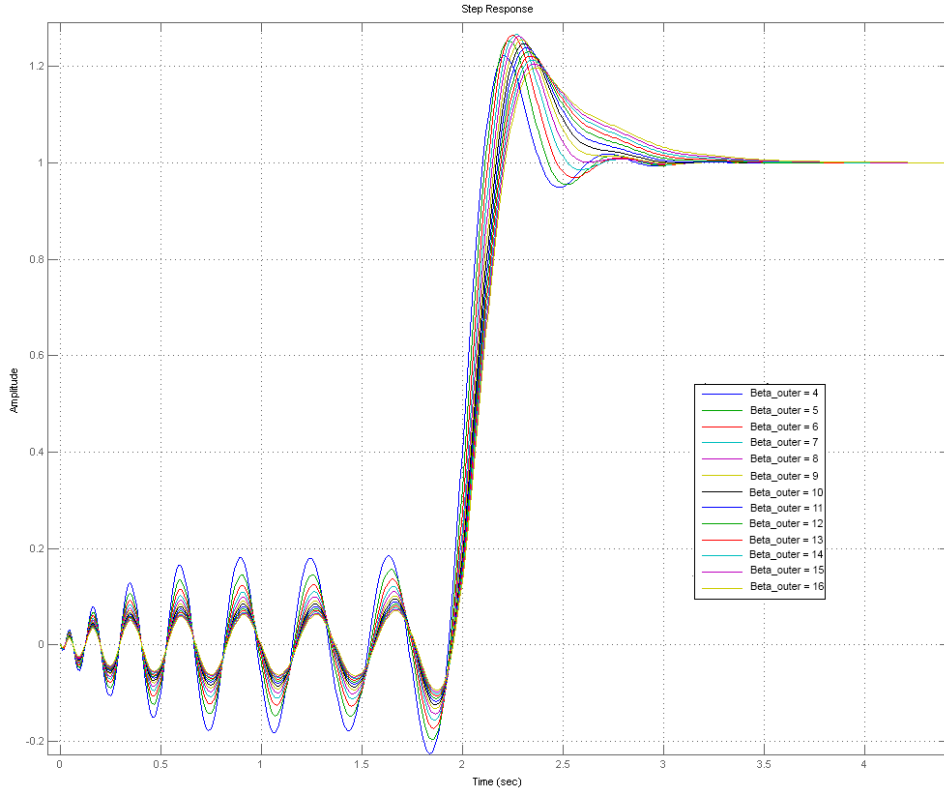| $O(\text{Padé})$	$A_{\max}$	Overshoot	Settling time
1	95.3%	0%	4.58 s
3	50.6%	2%	3.19 s
5	32.5%	6%	3.04 s
7	25.1%	12%	2.83 s
9	17.4%	17%	2.71 s
11	14.8%	21%	2.64 s
13	12.2%	24%	2.61 s
15	**10%**	**25%**	**2.60 s**
17	8.6%	27%	2.67 s
19	7.2%	27%	2.69 s
21	6.2%	28%	2.71 s

Figure 7: Kessler's method employed with Smith predictor for large latencies. The β_{Outer} control parameter's effect in the oscillation in the hold phase.

teleoperation with 2 s latency has been derived: $\beta_{\text{Outer}} = 6$ and $\beta_{\text{Outer}} = 9$ result in a system with $\tau = 2.61$ s and $\sigma = 25\%$, while the initial oscillation does not exceed 10%. The controller's parameters for $\beta_{\text{Outer}} = [4 \ldots 16]$ are:

- $k_{\text{Contr\_out}} = 157.448 \ldots 19.681$,

- $T_{\text{C1\_out}} = 0.05$,

- $T_{\text{C2\_out}} = 0.113 \ldots 0.451$.

5.5 PID–fuzzy controller

Accepting that the controller in the outer loop is a PID controller with the transfer function:

$$W_{\text{Contr\_out}} = \frac{k_{\text{Contr\_out}}}{s}(1 + sT_{\text{C1\_out}})(1 + sT_{\text{C2\_out}}), \tag{5.39}$$

the outer loop controller can be decomposed as the following series connection of proportional-integral (PI) and proportional-derivative (PD) blocks with the transfer functions W_{PI} and W_{PD}, respectively:

$$W_{\text{Contr\_out}} = W_{\text{PI}}W_{\text{PD}}, \tag{5.40}$$

$$W_{\text{PI}} = \frac{k_{\text{Contr\_out}}}{s}(1 + sT_{\text{C1\_out}}) \text{ and} \tag{5.41}$$

$$W_{\text{PD}} = 1 + sT_{\text{C2\_out}}. \tag{5.42}$$

Table 5: Effect of β_{Outer} on control parameters for Case 3 system design.

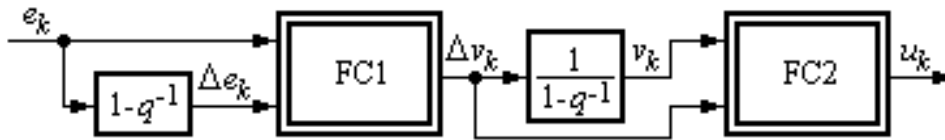| β_{Outer}	$A_{\max}$	Overshoot	Settling time
4	18.4%	22%	2.58 s
5	15.7%	25%	2.61 s
6	13.6%	26%	2.62 s
7	12.1%	27%	2.49 s
8	11%	25%	2.54 s
9	**10%**	**25%**	**2.61 s**
10	9.5%	24%	2.79 s
11	8.9%	23%	2.85 s
12	8.5%	22%	2.9 s
13	8%	21%	2.95 s
14	7.7%	20%	3 s
15	7.4%	20%	3.06 s
16	7.1%	19%	3.14 s

Figure 8: Structure of PID–fuzzy controller.

The structure of the PID–fuzzy controller is presented in Fig.8, where the nonlinear blocks FC1 and FC2 include the scaling of inputs and output, q^{-1} is the backward shift operator, e_k is the control error, $\Delta e_k = e_k - e_{k-1}$ is the increment of control error, v_k is an additional variable, and u_k is the control signal. The nonlinear block FC1 corresponds to W_{PI} and the nonlinear block FC2 corresponds to W_{PD}.

The two blocks FC1 and FC2 are characterized by the input membership functions presented in Fig.9. The inference engines of FC1 and FC2 employ the SUM and PROD operators assisted by the rule bases presented in Fig.10 and Fig.11, respectively. The weighted area method is used for defuzzification as FC1 and FC2 are Takagi–Sugeno fuzzy systems. The output of FC1 is fuzzified in order to be applied as input to FC2.

The rule consequents presented in Fig. 10 and Fig. 11 represent the discrete-time versions of nine separately designed PI and PID controllers. They are tuned using the results presented in the previous section and Tables 2-5, our PID–fuzzy controllers will behave like a bumpless interpolator between several separately tuned linear PID controllers. The separately tuned PID controllers are set such that to combine the advantageous performance of all PID controllers.
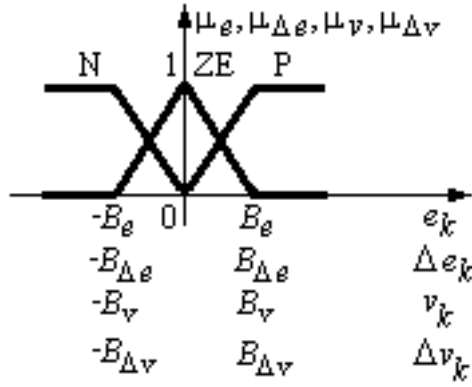
Figure 9: Input membership functions of FC1 and FC2.

$\dfrac{\Delta e_k}{e_k}$	N	ZE	P
P	$\Delta v_k = K^1_{P,PI}(\Delta e_k + \alpha^1_{PI} e_k)$	$\Delta v_k = K^2_{P,PI}(\Delta e_k + \alpha^2_{PI} e_k)$	$\Delta v_k = K^3_{P,PI}(\Delta e_k + \alpha^3_{PI} e_k)$
ZE	$\Delta v_k = K^4_{P,PI}(\Delta e_k + \alpha^4_{PI} e_k)$	$\Delta v_k = K^5_{P,PI}(\Delta e_k + \alpha^5_{PI} e_k)$	$\Delta v_k = K^6_{P,PI}(\Delta e_k + \alpha^6_{PI} e_k)$
N	$\Delta v_k = K^7_{P,PI}(\Delta e_k + \alpha^7_{PI} e_k)$	$\Delta v_k = K^8_{P,PI}(\Delta e_k + \alpha^8_{PI} e_k)$	$\Delta v_k = K^9_{P,PI}(\Delta e_k + \alpha^9_{PI} e_k)$

Figure 10: Rule base expressed as decision table of FC1.

$\dfrac{\Delta v_k}{v_k}$	N	ZE	P
P	$u_k = K^1_{P,PD}(\Delta v_k + \alpha^1_{PD} v_k)$	$u_k = K^2_{P,PD}(\Delta v_k + \alpha^2_{P2} v_k)$	$u_k = K^3_{P,PD}(\Delta v_k + \alpha^3_{PD} v_k)$
ZE	$u_k = K^4_{P,PD}(\Delta v_k + \alpha^4_{PD} v_k)$	$u_k = K^5_{P,PD}(\Delta v_k + \alpha^5_{PD} v_k)$	$u_k = K^6_{P,PD}(\Delta ve_k + \alpha^6_{PD} v_k)$
N	$u_k = K^7_{P,PD}(\Delta v_k + \alpha^7_{PD} v_k)$	$u_k = K^8_{P,PD}(\Delta v_k + \alpha^8_{PD} v_k)$	$u_k = K^9_{P,PD}(\Delta v_k + \alpha^9_{PD} v_k)$

Figure 11: Rule base expressed as decision table of FC2.

Tustin's method applied to the transfer functions defined in (5.42) leads to the following expressions of the parameters in Fig.10 and Fig.11:

$$K^i_{\text{P,PI}} = k^i_{\text{Contr\_out}} \left[1 - T_s/(2T^i_{\text{C1\_out}}) \right], \tag{5.43}$$

$$\alpha^i_{\text{PI}} = 2T_s/(2T^i_{\text{C1\_out}} - T_s), \tag{5.44}$$

$$K^j_{\text{P,PD}} = 1 - T_s/(2T^i_{\text{C2\_out}}), \tag{5.45}$$

$$\alpha^j_{\text{PD}} = 2T_s/(2T^i_{\text{C2\_out}} - T_s) \text{ where} \tag{5.46}$$

$$i, j = \overline{1, 9}, \tag{5.47}$$

where T_s is the sampling period, and $i, j = \overline{1, 9}$ are the current indexes of the PI and PD blocks. The parameters of the PID–fuzzy controllers are obtained in accordance with the following tuning condition:

$$B_{\Delta e} = B_e \left[\min(\alpha^1_{\text{PI}}, \ldots, \alpha^9_{\text{PI}}) \right], \tag{5.48}$$

$$B_{\Delta \nu} = B_\nu \left[\min(\alpha^1_{\text{PD}}, \ldots, \alpha^9_{\text{PD}}) \right]. \tag{5.49}$$

The tuning condition (5.49) ensures the modal equivalence, and the parameters B_e and B_v must be set by the designer. The stability analysis of the fuzzy control system is important with this regard.

6 Conclusion

We proposed a cascade control structure based empirical controller design to address the challenges of a system with large and probably varying latencies. With robot assisted surgery, a shared control approach should be followed, integrating high-fidelity automated functions into the robot to extend the capabilities of the human surgeon through image processing and force sensing. This concept could be most beneficial for long duration on-orbit missions, primarily on board of the International Space Station (ISS). Teleoperation controller design has a huge role in providing the high quality control signals and sensory feedback to facilitate surgery over the time-delay network.

Classical control methods were investigated for telesurgery, assessing their robustness in a time delay system and a fuzzy controller for the outer loop has been suggested. We showed that empirical approach through extended Ziegler–Nichols method and straight application of Kessler's Extended Symmetrical Optimum method did not provide acceptable controller parameters even with low latencies. Even the stretched Kessler method failed to tolerate latencies above 0.5 s relying solely on its robustness. Through employing a Smith predictor with Kessler's extended method, we managed to achieve good control parameters for our teleoperational system model for up to 2 s of delay. Therefore our method could theoretically be applied to reach out to near Earth (on orbit) spacecrafts, and to support reliable teleoperation.

7 Future work

Many different solutions have been investigated for bilateral teleoperation scenarios (Hokayem and Spong, 2006), and an appropriate version of it could be implemented with our struc-

ture. Also, a more complex tissue model will be incorporated, based on (Misra, Ramesh and Okamura, 2008). Other algorithms like soft-computing (hybrid fuzzy controller) is planned to be used in the outer control loop (Precup and Preitl, 2007). Time varying latency in today's internet network represent further technological challenges that need to be addressed (Sankaranarayanan, Potter and Hannaford, 2007).

Acknowledgment

References

Alvarez-Aguirre, A. 2010. *Predictor Based Control Strategy for Wheeled Mobile Robots Subject to Transport Delay*, IN-TECH, Ch. 3 in N. Mollet, Ed., *Remote and Telerobotics*, Vienna, pp. 33–59.

Arcara, P. and Melchiorri, C. 2002. Control schemes for teleoperation with time delay: A comparative study, *Robotics and Autonomous Systems* **38**: 49–64.

Astrom, K. and Hagglund, T. 1995. *PID controllers: theory, design, and tuning*, 2nd edn, Instrument Society of America, USA.

Brouwer, I., Ustin, J., Bentley, L., Sherman, A., Dhruv, N. and Tendick, F. 2001. Measuring in vivo animal soft tissue properties for haptic modeling in surgical simulation, *Proc. of the Medicine Meets Virtual Reality (MMVR8)*, Long Beach, pp. 69–74.

Enee, G. and Peroumalnaik, M. 2008. Adapted Pittsburgh classifier system: Applying reinforcement learning techniques to meteorological forecasting, *Intl. J. of Artificial Intelligence* **1**(A08): 96–110.

Fitts, P. 1992. The information capacity of the human motor system in controlling the amplitude of movement. 1954., *J. of Experimental Psychology: General* **121**(3): 262–269.

Fung, Y. 1990. *Biomechanics: Motion, Flow, Stress, and Growth*, Springer-Verlag, New York.

Haidegger, T. and Benyó, Z. 2007. Future of Surgical Robots in Space, *Proc. of the 58th Intl. Astronautical Congress (IAC)*, Hyderabad, pp. 1461–1471.

Haidegger, T. and Benyo, Z. 2008. Surgical robotic support for long duration space missions, *Acta Astronautica* **63**(7-10): 996–1005.

Haidegger, T., Kovács, L., Preitl, S., Precup, R.-E., Kovács, A., Benyó, B. and Benyó, Z. 2010a. Modeling and Control Aspects of Long Distance Telesurgical Applications, *Proc. of the*

IEEE Intl. Joint Conf. on Computational Cybernetics and Technical Informatics (ICCC-CONTI), Timisoara, pp. 197–202.

Haidegger, T., Kovács, L., Preitl, S., Precup, R., Kovács, A., Benyó, B. and Benyó, Z. 2010b. Cascade Control for Telehealth Applications, *Scientific Bulletin of The "Politehnica" University of Timisoara, Romania, Transactions on Automatic Control and Computer Science* **55(69)**(4): 99–108.

Hildo, Bijl 2006. Human–Machine Systems, Summary, *Course materials, Technical University of Delft*, available: www.aerostudents.com, pp. 1–19.

Hirzinger, G., Heindl, J. and Landzettel, K. 1989. Predictive and knowledge-based telerobotic control concepts, *Proc. of the IEEE Intl. Conf. on Robotics and Automation (ICRA)*, Scottsdale, pp. 1768–1777.

Hokayem, P. and Spong, M. 2006. Bilateral teleoperation: An historical survey, *Automatica* **42**(12): 2035–2057.

Joelianto, E., W. S. and Ichsan, M. 2009. Time series estimation on earthquake events using ANFIS with mapping function, *Intl. J. of Artificial Intelligence* **3**(A09): 37–63.

Kawashima, K., Tadano, K., Sankaranarayanan, G. and Hannaford, B. 2008. Model-based passivity control for bilateral teleoperation of a surgical robot with time delay, *IEEE/RSJ Intl. Conf. on Intelligent Robots and Systems (IROS)* pp. 1427–1432.

Kessler, C. 1958. Das Symmetrische Optimum, *Regelungstechnik* **6**: 395–400, 432–436.

Lantos, B. 2001. *Theory and design of control systems I-II*, Akademia Press, in Hungarian, Budapest.

McRuer, D. 1995. *Pilot-induced oscillations and human dynamic behavior*, PhD thesis, NASA.

McRuer, D. and Jex, H. 1967. A Review of Quasi-Linear Pilot Models, *IEEE Trans. on Human Factors in Electronics* **8**(3): 231–249.

Misra, S., Ramesh, K. and Okamura, A. 2008. Modeling of Tool-Tissue Interactions for Computer-Based Surgical Simulation: A Literature Review, *Presence (Cambridge)* **17**(5): 463–491.

Precup, R. and Preitl, S. 2007. PI-Fuzzy controllers for integral plants to ensure robust stability, *Information Sciences* **177**(20): 4410–4429.

Preitl, S. and Precup, R. 1999. An extension of tuning relations after symmetrical optimum method for PI and PID controllers, *Automatica* **35**(10): 1731–1736.

Preitl, S. and Precup, R. 2000. Extended Symmetrical Optimum (ESO) Method: A New Tuning Strategy for PI/PID Controllers, *Proc. of the IFAC Workshop on Digital Control: Past, Present and Future of PID Control*, number 1, pp. 421–426.

Preitl, S. and Precup, R. 2003. Points of View in Controller Design by Means of Extended Symmetrical Optimum Method, *Proc. of the IFAC Control Systems Design (CSD)*, Brastislava, pp. 95–100.

Preitl, S., Precup, R., Kovacs, L. and Preitl, Z. 2002. Control Solutions for Electrical Driving Systems . Tuning Methodologies for PI and PID Controllers, *Proc. of the Kandó Conf. 2002—60 years in Electrical Training*, BMF, Budapest.

Rayman, R., Croome, K., Galbraith, N., McClure, R., Morady, R., Peterson, S., Smith, S., Subotic, V., Wynsberghe, A. V. and Primak, S. 2006. Long-distance robotic telesurgery: a feasibility study for care in remote environments, *Intl. J. of Medical Robotics and Computer Assisted Surgery* **2**(3): 216–224.

Rayman, R., Primak, S., Patel, R., Moallem, M., Morady, R., Tavakoli, M., Subotic, V., Galbraith, N., van Wynsberghe, A. and Croome, K. 2005. Effects of latency on telesurgery: an experimental study, *Lecture Notes in Computer Science (LNCS), Proc. of the Annual Conf. of the Medical Image Computing and Computer Assisted Intervention Society (MICCAI)*, Vol. 3750, Springer, Palm Springs, pp. 57–64.

Sankaranarayanan, G., Potter, L. and Hannaford, B. 2007. Measurement and Emulation of Time Varying Packet Delay with Applications to Networked Haptic Virtual Environments, *ACM International Conference Proceeding Series, 1st Intl. Conf. on Robot Communication and Coordination (ROBOCOMM)*, Vol. 318, Athens.

Thompson, J., Ottensmeyer, M. and Sheridan, T. 1999. Human factors in telesurgery: effects of time delay and asynchrony in video and control feedback with local manipulative assistance., *Telemedicine Journal: the official journal of the American Telemedicine Association* **5**(2): 129–37.

Vrancic, D., Strmcnik, S. and Juricich, J. 2001. A magnitude optimum multiple integration tuning method for filtered PID controller, *Automatica* **37**(9): 1473–1479.

Zhao, Z.-Y., X. W.-F. and Hong, H. 2010. Hybrid optimization method of evolutionary parallel gradient search, *Intl. J. of Artificial Intelligence* **5**(A10): 1–16.

Ziegler, J. and Nichols, N. 1942. Optimum settings for automatic controllers, *Trans. of the ASME* **64**: 759–768.